Article

Antiviral Potential of Selected *N*-Methyl-*N*-phenyl Dithiocarbamate Complexes against Human Immunodeficiency Virus (HIV)

Hazel T. Mufhandu [1,*], Oluwafemi S. Obisesan [1], Timothy O. Ajiboye [2], Sabelo D. Mhlanga [2] and Damian C. Onwudiwe [3,4,*]

[1] Department of Microbiology, School of Biological Sciences, Faculty of Natural and Agricultural Sciences, North-West University, Mafikeng Campus, Private Bag X2046, Mmabatho 2735, South Africa; successfreak01@gmail.com

[2] Chemistry Department, Nelson Mandela University, University Way, Summerstrand, Gqeberha 6019, South Africa; timaji2003@gmail.com (T.O.A.); sabelo.mhlanga@mandela.ac.za (S.D.M.)

[3] Material Science Innovation and Modelling (MaSIM) Research Focus Area, Faculty of Natural and Agricultural Sciences, North-West University, Mafikeng Campus, Private Bag X2046, Mmabatho 2735, South Africa

[4] Department of Chemistry, School of Physical and Chemical Sciences, Faculty of Natural and Agricultural Sciences, North-West University, Mafikeng Campus, Private Bag X2046, Mmabatho 2735, South Africa

* Correspondence: hazel.mufhandu@nwu.ac.za (H.T.M.); damian.onwudiwe@nwu.ac.za (D.C.O.)

Abstract: Despite the use of highly active antiretroviral therapy approved by the United States Food and Drug Administration (FDA) for the treatment of human immunodeficiency virus (HIV) infection, HIV remains a public health concern due to the inability of the treatment to eradicate the virus. In this study, *N*-methyl-*N*-phenyl dithiocarbamate complexes of indium(III), bismuth(III), antimony(III), silver(I), and copper(II) were synthesized. The complexes were characterized by thermal gravimetric analysis (TGA), differential scanning calorimetry (DSC), and Fourier transform infrared spectroscopy (FTIR). The *N*-methyl-*N*-phenyl dithiocarbamate complexes were then evaluated for their antiviral effects against HIV-1 subtypes A (Q168), B (QHO.168), and C (CAP210 and ZM53). The results showed that the copper(II)-bis (*N*-methyl-*N*-phenyl dithiocarbamate) complex had a neutralization efficiency of 94% for CAP210, 54% for ZM53, 45% for Q168, and 63% for QHO.168. The silver(I)-bis (*N*-methyl-*N*-phenyl dithiocarbamate) complex showed minimal neutralization efficiency against HIV, while indium(III) and antimony(III) *N*-methyl-*N*-phenyl dithiocarbamate complexes had no antiviral activity against HIV-1. The findings revealed that copper(II)-bis (*N*-methyl-*N*-phenyl dithiocarbamate), with further improvement, could be explored as an alternative entry inhibitor for HIV.

Keywords: dithiocarbamate complexes; human immunodeficiency virus; cytotoxicity; antiviral efficacy; pseudovirus; inorganic compounds

1. Introduction

The United Nation Member States have agreed on the approach to end AIDS by 2030, but this cannot be achieved without innovative antiretroviral drugs and HIV treatment formulations [1]. This is particularly important given the alarming statistics of HIV-infected people released by the World Health Organization. It has been estimated that 1.5 million, 360,000, 2.4 million, 3.5 million, 3.3 million, and 26 million people living in the western Pacific, the eastern Mediterranean, Europe, Southeast Asia, the Americas, and Africa, respectively, are infected with HIV, indicating that 75 million people are infected globally [2]. The use of highly active antiretroviral therapy (HAART) in the treatment of HIV has transformed the course of disease progression from what was initially considered as a death sentence to a more treatable infection [3]. The HAART treatment involves the use of

multiple antiretroviral drugs to stop HIV from progressing into AIDS [4]. Most HAART regimens administered for HIV treatment consist of three or more antiretroviral drugs (two nucleoside or nucleotide reverse transcriptase inhibitors and one non-nucleoside reverse transcriptase inhibitor/protease inhibitor). However, the adverse effects of the drugs may also affect the quality of life of the patients [5,6]. To bring an end to HIV and AIDS, several compounds have been used as antiviral agents. For instance, biosynthesized zinc oxide, metallic gold, and metallic silver nanoparticles have been examined as antiviral agents against HIV [7]. Soundararajan et al. reviewed different polymeric [poly(lactide-*co*-glycolide), poly(L-lactic acid), poly(ethylene oxide), poly(caprolactone), and sodium poly(styrene-1-sulphonate)], dendrimer (polyanionic carbosilane and PEGylated-PAMAM), and biomacromolecule (chitosan-based micellar system) nanoparticle-based compounds that have been used as antiviral agents against HIV [8]. Apart from nanoparticles, different medicinal plants have been investigated for the treatment of HIV [9,10]. The root bark, stem bark, leaf, and entire root of plants such as *Erythrina abyssinica* Lam, *Spathodea campanulata* P. Beauv., *Hoslundia opposita* Vahl, *Bidens pilosa* L., *Artemisia annua* L., *Calendula officinalis* L., and *Piptadeniastrum africanum* (Hook. f.) Brenan [2,11]. The limitation to the use of some plants as anti-HIV agents is their phytotoxic nature [12]. Plants such as *Mangifera indica*, *Moringa oleifera*, and *Spirulina platensis* are, however, used for ameliorating metabolic syndrome (MetS) for patients subjected to HAART [13–15].

In addition to the use of plants, different inorganic complexes have also been investigated for the inhibition of HIV, such as vanadium complexes with different ligands. The oxovanadium(IV) porphyrin complexes have demonstrated better antiviral activities than vehicle control. Their inhibitory effect was particularly noted in the Hut/CCR5 cells, and there was more than 97% inhibition of these cells. As revealed by the molecular modeling simulation, the oxovanadium(IV) porphyrins displayed better binding to the CD4 protein. In short, the action of these complexes against HIV is that they block the virus from reaching the host cells which are the target [4]. Some inorganic complexes have been investigated for HIV treatment due to their antiproliferative (cytostatic) properties. The cytostatic drugs will not impact the invading pathogens; rather, they affect the host cells and, in most cases, are used along with other antiviral agents. Examples of cytostatic inorganic complexes include some of the gold(III) complexes. For instance, when four bis(thiosemicarbazonate)gold(III) complexes were investigated for HIV treatment, at a non-toxic concentration of 12.5 μM, one of these complexes displayed 98% inhibition of viral infection of TZM-bl cells with $IC_{50} = 6.8 \pm 0.6$ μM, while the other showed 72% inhibition ($IC_{50} = 5.3 \pm 0.4$ μM) at 6.25 μM [16]. Other complexes that have been investigated for HIV treatment are terpyridyl Ru(II) complex [1], aminothiazole compounds [17,18], and polypyridyl Ru(II) complexes [19]. Through the use of all these complexes and plant products, drugs such as efavirenz, dolutegravir, elvitegravir, raltegravir, darunavir, and rilpivirine emerged for the management of HIV.

The use of different dithiocarbamate compounds as HIV inhibitors has also been reported [20,21]. In a phase II trial, the exposure of HIV to disulfiram led to a change in the RNA of HIV as shown by the polymerase chain reaction (PCR), which suggests that dithiocarbamate-based drugs might be a future cure for HIV [22]. Another dithiocarbamate compound that has been used for clinical trials is copper-chelating diethyldithiocarbamate. It showed a notable delay in slowing down the progression of HIV-1 to AIDS [23]. Some other dithiocarbamate compounds that have been investigated are zinc-dithiocarbamate-*S*,S′-dioxide, zinc-dithiocarbamate-*S*,S′-dioxidcyclic, diethyldithiocarbamate, and pyrrolidine dithiocarbamate. These compounds act by either inhibiting nuclear factor-κB, blocking the activation of HIV-1, or mediating a cell-to-cell fusion between anti-CXCR4 and CXCR4 [23–26]. There is no report on the use of *N*-methyl-*N*-phenyl dithiocarbamate as an inhibitor of HIV. Hence, the present investigation focuses on the assessment of *N*-methyl-*N*-phenyl dithiocarbamate for the treatment of HIV. The structures of some of the investigated complexes are shown in Figure 1.
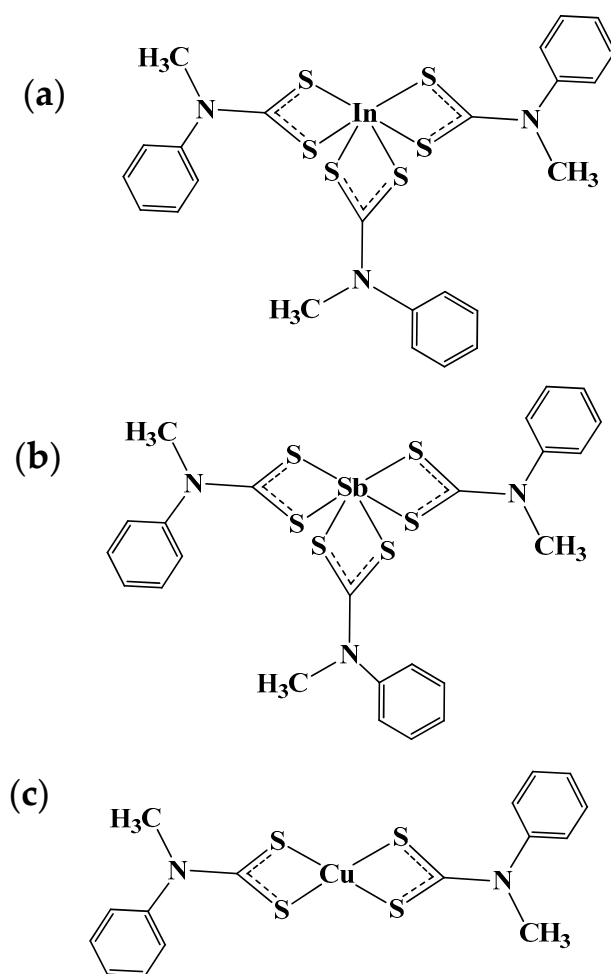
Figure 1. Structures of some of the *N*-methyl-*N*-phenyl dithiocarbamate complexes selected for the investigations. (**a**) Indium(III)-tris (*N*-methyl-*N*-phenyl dithiocarbamate). (**b**) Antimony(III)-tris (*N*-methyl-*N*-phenyl dithiocarbamate). (**c**) Copper(II)-bis (*N*-methyl-*N*-phenyl dithiocarbamate) complexes.

2. Experimental Design

2.1. Materials and Physical Measurements

All solvents and reagents used were of analytical grade, and no additional purification was required. The IR spectra were measured using a Bruker IFS 66v/S in the range of 4000–400 cm^{-1}, and the thermal stability studies were conducted using thermal gravimetric analysis/differential scanning calorimetry (TGA-DSC) (Mettler-Toledo GmbH, Gieβen, Germany).

2.2. Synthesis of N-Methyl-N-phenyl Dithiocarbamate Ligand and Complexes

2.2.1. Synthesis of Ammonium *N*-Methyl-*N*-phenyl Dithiocarbamate Ligand

The ligand was prepared through a synthetic procedure already established in the literature with slight modification [27–30]. In brief, 22 mL of N-methyl aniline was mixed with 62 mL of concentrated aqueous ammonia in ice. Then, 10 mL of ice-cold carbon disulphide was added dropwise with constant stirring. The stirring of the entire contents continued for 9 h. There was a formation of a light-yellow precipitate. The precipitate was washed with cold methanol and filtered under pressure to remove the solvents. To prevent the decomposition of the synthesized ligands, the product was immediately kept inside the refrigerator. The mechanism of the reaction is summarized in Figure 2.
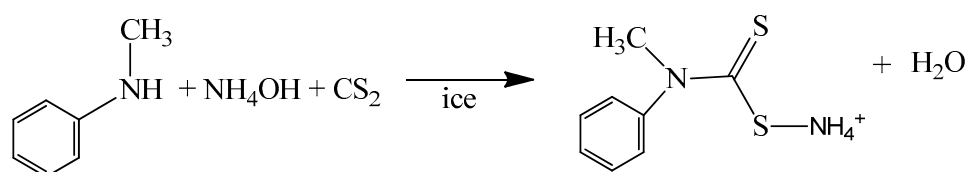
Figure 2. Mechanism of *N*-methyl-*N*-phenyl dithiocarbamate ligand formation.

2.2.2. Synthesis of the Complexes

The prepared ammonium *N*-methyl-*N*-phenyl dithiocarbamate ligand was reacted with stoichiometric equivalence of the metal salt of antimony, indium, copper, silver, and bismuth and was stirred for one hour. Colored precipitates were separated from the reaction solution by filtration, rinsed thoroughly with a water/ethanol mixture (50:50), and dried.

2.3. Cells, Envelope Plasmids, Reagents, and Chemical Inhibitors

TZM-bl cells were used for virus titration and neutralization assay while the HEK 293T cells were used for virus transfection. Both cell lines were cultured in Dulbecco's modified Eagle medium (DMEM), (Thermofisher Scientific, Waltham, MA, USA) supplemented with heat-inactivated 10% fetal bovine serum (FBS) (Gibco, Thermofisher, Waltham, MA, USA), 1% L-glutamine 200 Mm (Sigma-Aldrich, St. Louis, MO, USA), penicillin (100 IU/mL) and streptomycin (100 μg/mL) (Sigma-Aldrich, St. Louis, MO, USA), and 1% non-essential amino acids (NEAA) (Sigma-Aldrich, St. Louis, MO, USA) in a humidified environment at 37 °C, 5% CO_2. HIV-1 envelope (Env)-expression plasmids (pcDNA 3.1-*gp 160*) with different HIV-1 gp160 inserts of subtypes A (Q168), B (QHO.168), and C (CAP210 and ZM53) and the Env-deficient HIV-1 backbone vector (pSG3Env) were obtained as gifts from the NextGen Research Unit at the Council for Scientific and Industrial Research (CSIR, South Africa). MTT reagent (3-(4,5-dimethylthiazol-2-yl)-2,5-diphenyl tetrazolium bromide) and neutral red dye (3-amino-7-dimethylamino-2-methyl-phenazine hydrochloride) were purchased from Promega (Anatech, Randburg, South Africa). Chemical inhibitors synthesized from *N*-methyl-*N*-phenyl dithiocarbamate complexes of five inorganic compounds, silver(I), bismuth(III), copper(II), indium(III), and antimony(III), were used as test compounds. Tenofovir disoproxil fumarate (TDF), an FDA-approved drug purchased from DB Fine Chemicals (Sandton, South Africa), and anti-HIV-1 gp120 monoclonal antibody (Aalto Bio Reagents, Dublin, Ireland) were used as positive controls in the study.

2.4. Generation of HIV-1 Env-Pseudoviruses

HIV-1 subtype A, B, and C Env pseudoviruses were generated as previously described by Li et al. [31], and the tissue culture infective dose ($TCID_{50}$) was determined as previously described [32]. The pseudoviruses were prepared by transfecting 293T cells (2.0×10^6) maintained in complete DMEM at 37 °C, 5% CO_2. The expression plasmid and the backbone vector at 1:2 dilutions were pre-incubated with X-tremeGENE 9 DNA transfection reagent (Merck, Darmstadt, Germany) at ambient temperature for 45 min to form a complex, which was added to the 293T cells and incubated for 48 h. The supernatant was harvested post-transfection and filtered using the 0.45 μm filters (Corning, Merck, Darmstadt, Germany) to remove the cell debris. The tissue culture infective dose ($TCID_{50}$) was determined as previously described [32]. That is, the virus titration of each batch of pseudovirus production was determined in TZM-bl cells as the $TCID_{50}$. Briefly, eleven dilution steps of fourfold dilutions of the pseudovirus were prepared in quadruplicate wells in a 96-well plate, 1×10^4 cells/100 μL was added to each well, and the plate was incubated for 48 h. The media were replaced with Bright Glo luciferase reagent (Promega, Madison, WI, USA) post-incubation, and the luminescence was determined using a luminometer (Perkin-Elmer Life Sciences, Waltham, MA, USA).

2.5. Cytotoxicity Assay

The cytotoxicity of the test chemical compounds, that is, *N*-methyl-*N*-phenyl dithio-carbamate complexes of silver(I), bismuth(III), copper(II), indium(III), and antimony(III), referred to as Ag(I)DT, Bi(III)DT, Cu(III)DT, In(III)DT, and Sb(III)DT, respectively, was determined in TZM-bl cells using two different in vitro cell viability assays, MTT and neutral red assays. The MTT cell viability assay was used to determine the metabolic response of active cells to the test compounds while the neutral red uptake assay was used to measure cell viability by determining the number of live cells that could retain the neutral red dye in their lysosomes through passive diffusion.

2.5.1. MTT Assay

The viability of the test compounds was determined using MTT assay as previously described [33]. In 96-well plates, 1×10^4 cells/100 µL were seeded per well (Corning-costar, Merck, Darmstadt, Germany) and incubated at 37 °C, 5% CO_2 for 24 h. Threefold serial dilutions of the compounds were prepared in media containing 0.1% dimethylsulphoxide (DMSO) for a working concentration of 11–0.002 µg/mL. Cells were treated with different concentrations of the compounds in triplicate and incubated for 48 h. The media were then removed, replaced with 25 µL MTT solution (5 mg/mL, Promega, Sigma-Aldrich, Madison, WI, USA), and incubated for 3 h. MTT solution was removed, and 100 µL of DMSO was added to the wells for crystal solubilization. The absorbance was measured at a wavelength of 570/620 nm using a microplate reader (Multiskan GO microplate spectrophotometer, ThermoScientific™, Porto Salvo, Portugal).

2.5.2. Neutral Red Uptake Assay

The neutral red uptake assay was conducted on the test compounds using a previously established protocol [34]. TZM-bl cells were seeded at a density of 1×10^4 cells/100 µL in a 96-well plate and incubated for 24 h. The same working concentration of the test compounds used for MTT was used for this assay. Cells were treated with different concentrations of the compounds in triplicate and incubated for 48 h. The media containing the test compounds were removed, and the cells were washed with pre-warmed phosphate-buffered saline (1x PBS, pH 7.4). About 200 µL of the neutral red solution was added to the wells at 37 °C, 5% CO_2 for 2 and a half hours. The neutral red solution was aspirated from the wells, and the cells were washed with PBS before desorption with 200 µL neutral red solubilization solution. The absorbance was recorded at a wavelength of 540/690 nm as above.

2.6. Neutralization Assay

The chemical compounds were tested for their inhibition efficiency against different subtypes of HIV-1 pseudoviruses in TZM-bl cells. This was performed using the single-round infection neutralization assay as previously described [35,36]. HIV inhibition was measured as a percentage reduction in the luciferase gene expression in Env-pseudotyped virus-infected cells. The anti-HIV-1 gp120 monoclonal antibody (gp120 mAb) was used as a positive control. The HIV-1 gp120 mAb is a synthetic protein designed to block HIV-1 entry via the gp120 subunit of the envelope glycoprotein. Specifically, triplicate runs of a 3-fold serial dilution of the chemical compounds and gp120 mAb were prepared in a growth medium at a starting concentration of 1.23 µg/mL and 100 µg/mL, respectively, and incubated with 50 µL pseudovirus (2×10^4 $TCID_{50}$) for 1 h at 37 °C, 5% CO_2. Then, 1×10^4 cells/100 µL were added to the wells and incubated for 48 h. The titer was determined as the half-maximal inhibitory concentration (IC_{50}) that reduced the relative light units (RLU) by half when compared to the virus control after subtracting the cell control background.

2.7. Statistical Analysis

The antiviral activity of the test compounds was measured against different subtypes of HIV-1 pseudoviruses. All experiments were conducted in triplicate. Data are presented as mean ± standard deviation (SD). Data analysis was performed using GraphPad Prism 9.0 (GraphPad Prism Software, Inc., San Diego, CA, USA). A one-way ANOVA analysis was used to determine the statistical significance. A *p*-value of <0.05 was considered statistically significant.

3. Results and Discussion

3.1. Fourier Transform Infrared Spectroscopy (FTIR) Analysis of the Complexes

The characteristic peak of dithiocarbamate group appeared in the fingerprint region on the spectra of the three complexes as shown in Figures 3–5. The stretching vibration of C-N and –CSS appears as two sharp peaks in the spectra around the 1000 cm^{-1} region while the stretching vibration of the C-N bond appears as a prominent peak around 1400 cm^{-1}. The peaks above 3000 cm^{-1} and around 700 cm^{-1} are for the aromatic ring stretching and bending of the C-H bond, respectively. The metal-sulphur peak (M-S) appears around 480 cm^{-1}, and the peak that is slightly above 1500 cm^{-1} is a characteristic peak of C=C of the aromatic structure. The C-H stretching vibration of the alkyl groups were identified around 3000 cm^{-1}. All these values are consistent with the values obtained from the literature [37,38]. In our previous studies, the characterization (including FTIR analysis) of silver(I) and bismuth(III) of *N*-phenyl-*N*-methyl dithiocarbamate has been discussed [39–41].
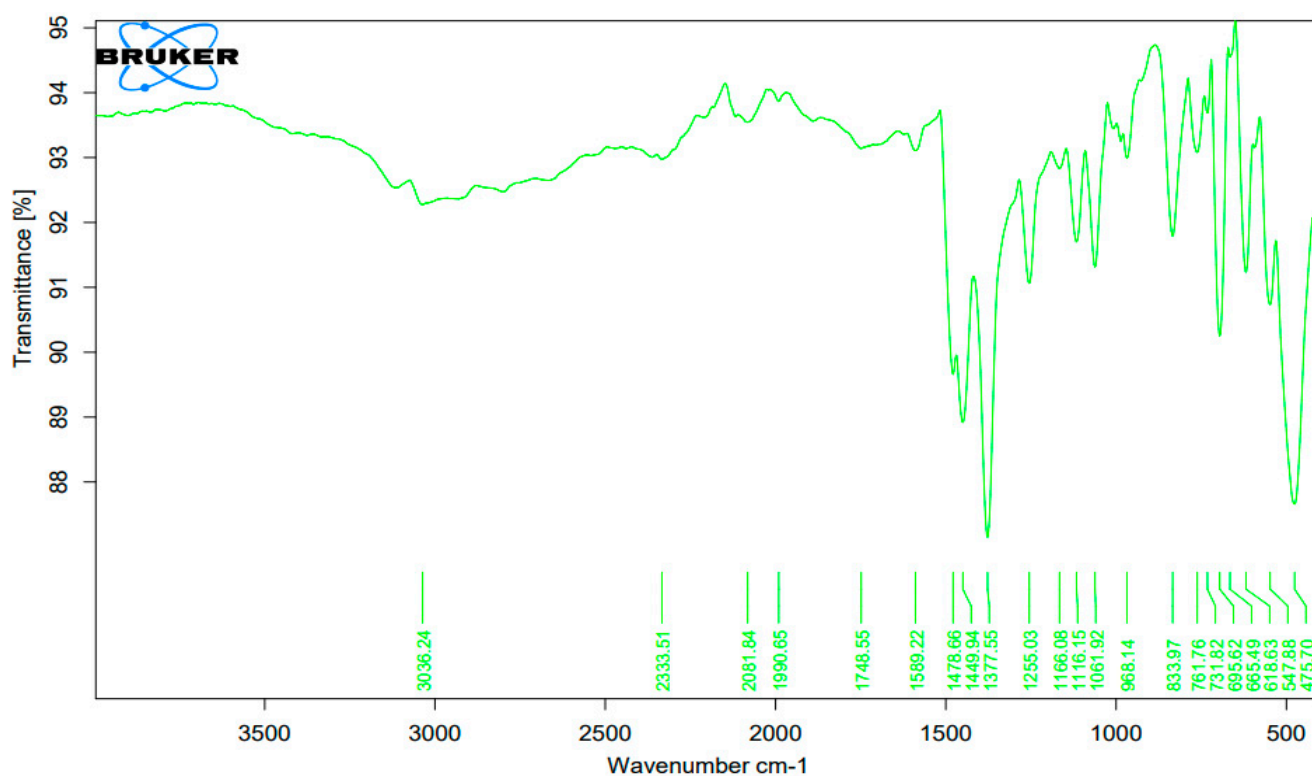

Figure 3. FTIR spectra of antimony(III)-tris (*N*-methyl-*N*-phenyl dithiocarbamate) complex.
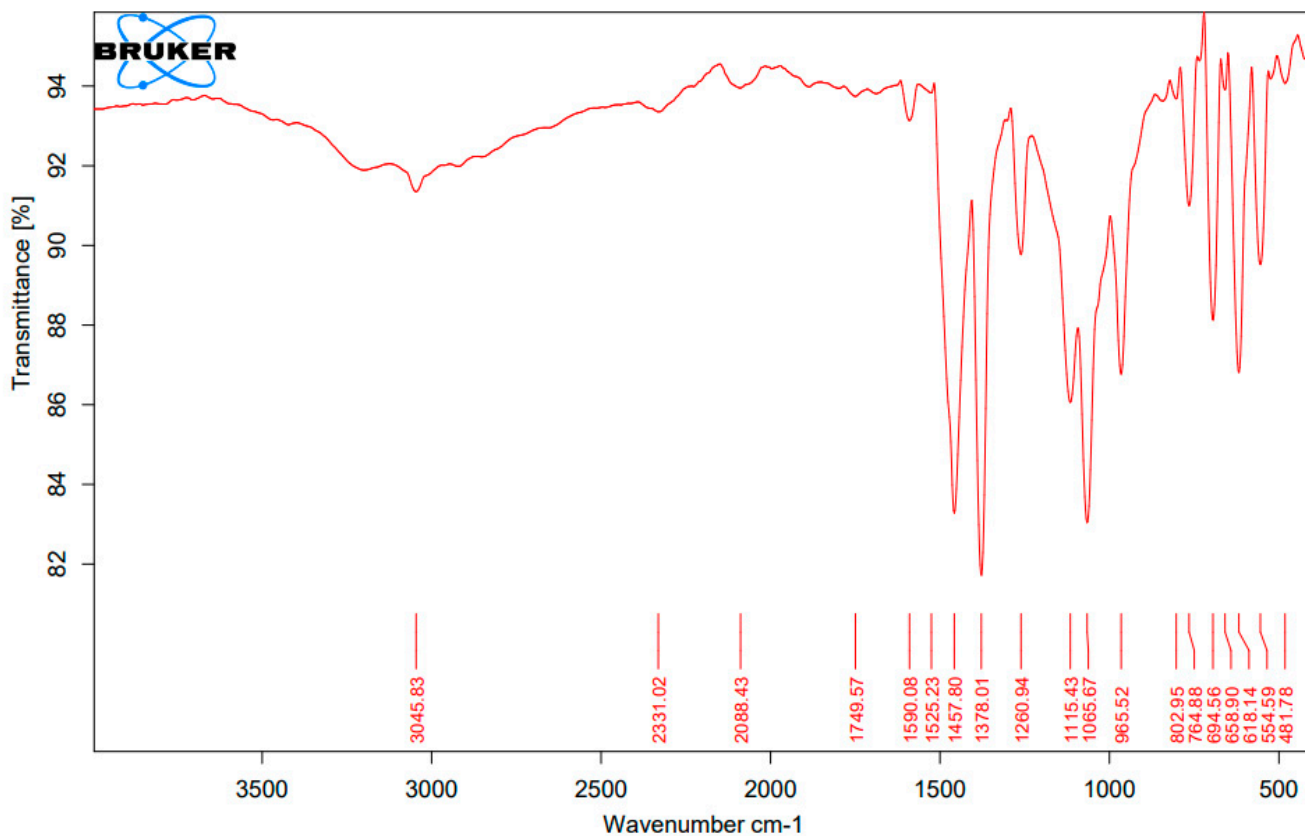
Figure 4. TIR spectra of indium(III)-tris(*N*-methyl-*N*-phenyl dithiocarbamate) complex.
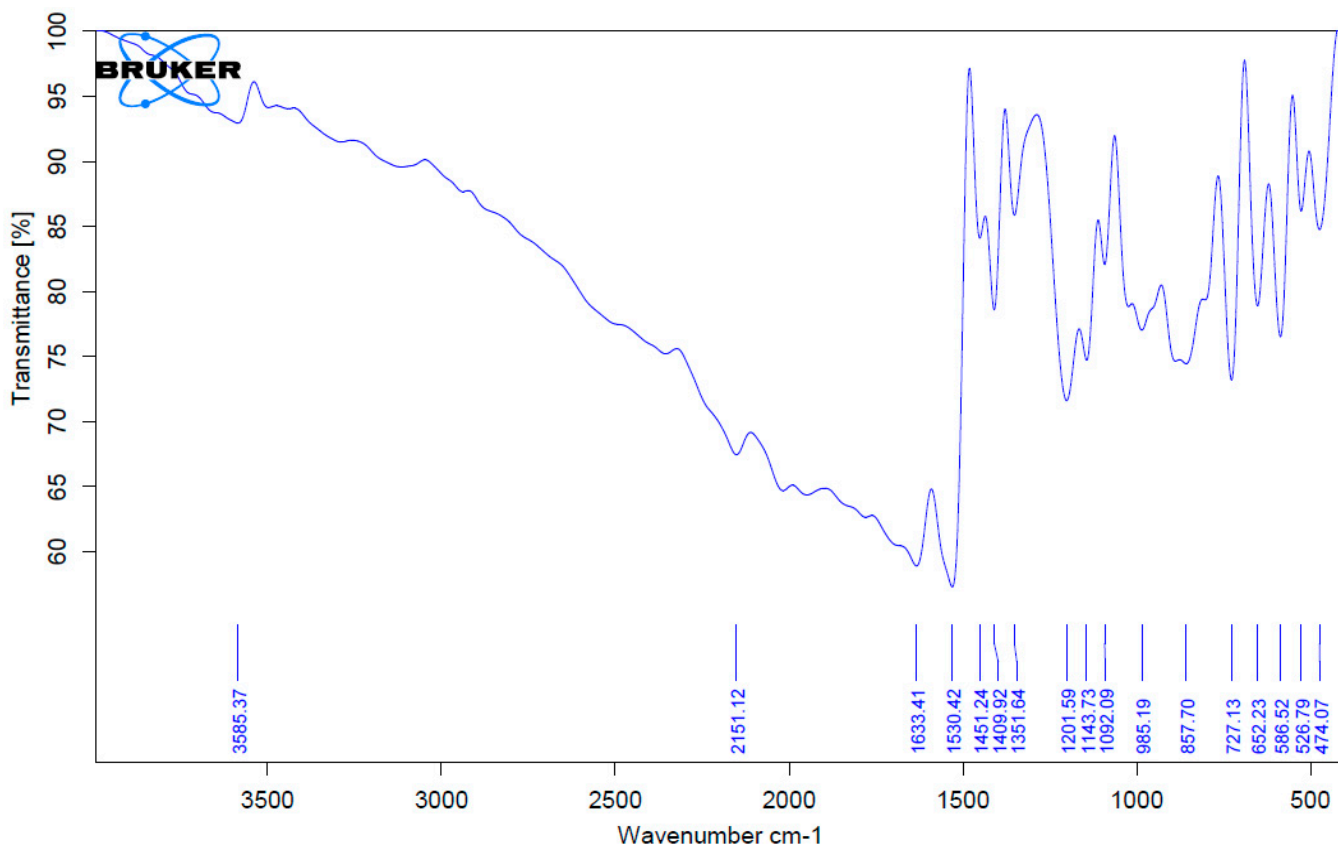

Figure 5. FTIR spectra of copper(II)-bis(*N*-methyl-*N*-phenyl dithiocarbamate) complex.

3.2. Thermal Analysis of the Complexes

The antimony, indium, and copper dithiocarbamate) complexes were heated from 0 to 600 °C under argon atmosphere with a flow rate of 75 mL/min. As shown in the thermal gravimetric analysis (TGA) thermograms in Figures 6–8, there was a loss in weight around 100 °C for the antimony complex, which could be a result of the loss of the water molecule present in the complex [42]. The water loss occurred at around 50 °C for the copper complex (2.67% weight loss) and slightly below 200 °C for the indium complex. This shows that the water molecule is tightly bound to the indium complex since its release required more thermal energy, while it is weakly held in the copper complex.
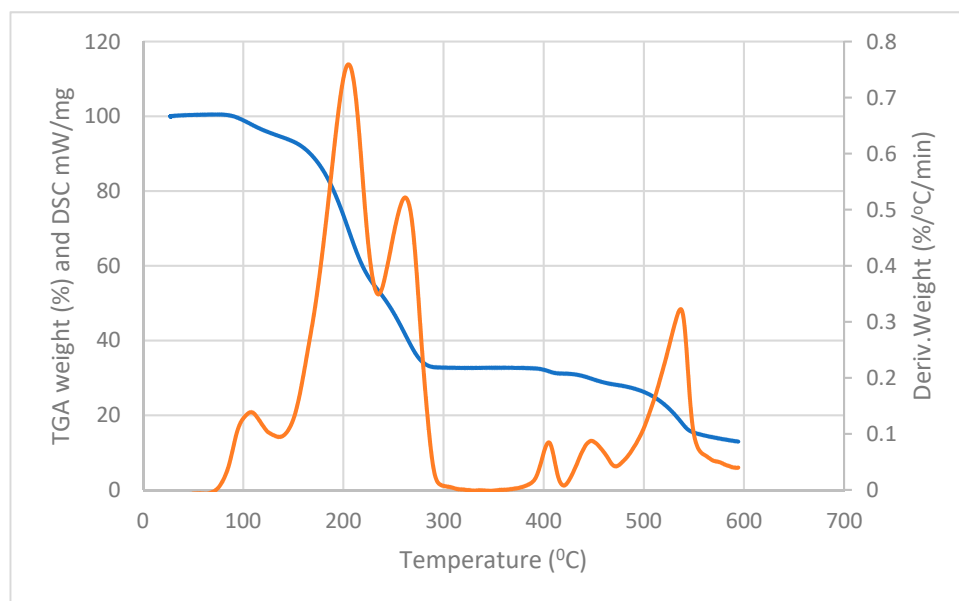

Figure 6. TGA and DSC plot of antimony(III) *N*-methyl-*N*-phenyl dithiocarbamate complex. The blue color is the TGA plot while the orange color is the DSC plot.
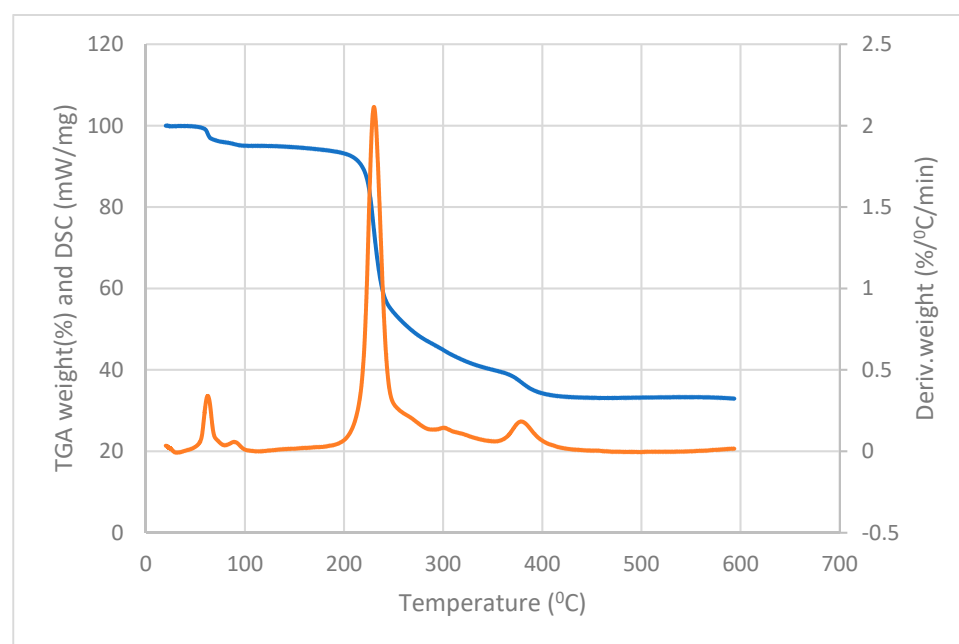

Figure 7. TGA and DSC plot of copper (II) *N*-methyl-*N*-phenyl dithiocarbamate complex. The blue color is the TGA plot while the orange color is the DSC plot.
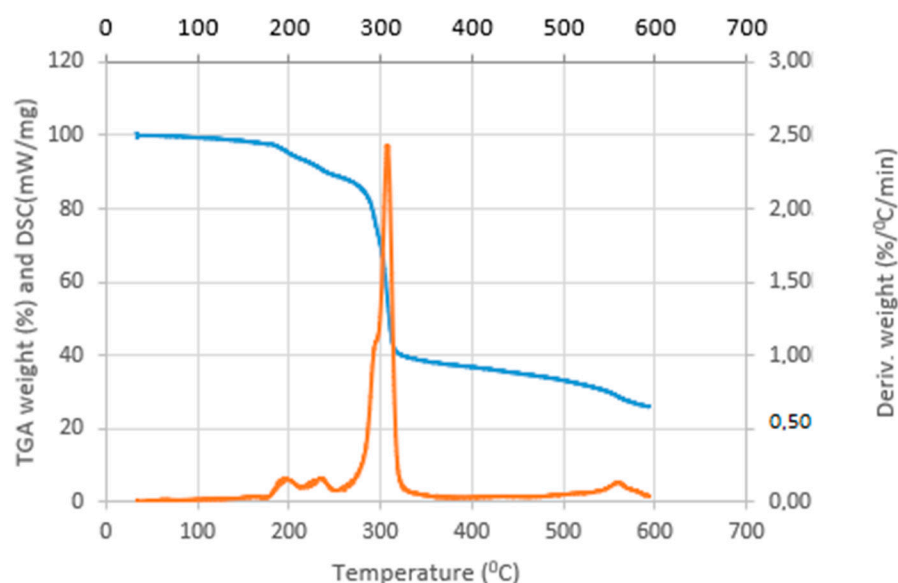
Figure 8. TGA and DSC plot of indium (III) *N*-methyl-*N*-phenyl dithiocarbamate complex. The blue color is the TGA plot while the orange color is the DSC plot.

Another pronounced loss in weight, common to the three complexes, is observed between 200 and 350 °C. It is in this range of temperature that the organic component of the complexes was decomposed, which was more than 50% of the starting material for each of the three complexes. The weight loss after 350 °C indicates the formation of metal sulphides due to higher residual weight [43]. This result indicates that the ligand was changed to the metal complex. The product of the decomposition of the copper complex is more stable than the one obtained from both the antimony and indium complexes. This was due to the percentage of residue left at 600 °C. The residual percentages were about 33, 26, and 13% for the copper complex, indium complex, and antimony complex, respectively, as shown in their TGA thermograms.

The differential scanning calorimetry (DSC) thermogram further revealed the formation of the complexes. One prominent endothermic peak is common to all the complexes, and each of the peaks appears between 200 and 309 °C. These endothermic peaks indicate that the melting point of all the complexes falls within the temperature range of 200–309 °C. Another endothermic peak that is common to all the complexes appears between 350–550 °C, which shows that all the complexes decomposed to give their corresponding sulphides. It is also evident that these complexes can be used for synthesizing the corresponding metal sulphides. This thermal behavior is similar to what has previous report on the decomposition of similar dithiocarbamate complexes [44–46]. Our previous studies also discussed the characterization (including thermal analysis) of silver(I) and bismuth(III) of *N*-phenyl-*N*-methyl dithiocarbamate [39–41].

3.3. Effects of Inorganic Dithiocarbamate Complexes on TZM-bl Cells

The cytotoxicity of five compounds of dithiocarbamate complexes, Ag(I)DT, Cu(II)DT, Bi(III)DT, In(III)DT, and Sb(III)DT, was assessed in TZM-bl cells to determine their safety. The effect of the compounds on TZM-bl cells was measured as percentage cell viability and was compared with the TDF positive control (Figure 9). Overall, the assays showed a decreasing order of cell viability of Cu(II)DT < Ag(I)DT < In(III)DT < Sb(III)DT < BI(III)DT < TDF. The cytotoxicity examined with the MTT assay showed that all the test compounds were non-toxic when used at concentrations of 0.002–1.23 µg/mL, with 80–130% cell viability. The increase in the percentage cell viability above 100% is suggestive of an active cell proliferation during the period of the experiment [47]. However, as the concentration increased (11 µg/mL), the viability of cells treated with Ag(I)DT and Cu(II)DT reduced to 25% and 14%, respectively. Similar results were observed with the neutral red uptake assay,

indicating increased cell viability as the concentrations of the test compounds decreased. This shows that an increased concentration of the compounds in the cells will cause the metabolic response and the structural integrity of the cells to be affected. The inhibitory effect of these compounds is responsible for the toxicity observed in the assay. In addition, the cells were viable at 80–130% after 48 h of incubation at a concentration of 11.1 µg/mL (Figure 9B), except for Ag(I)DT and Cu(II)DT which showed 19% and 18% viability, respectively. These two complexes showed toxicity to the cells at increased concentrations compared to Bi(III)DT, Sb(III)DT, and In(III)DT which were non-toxic to the cells at the same concentration.
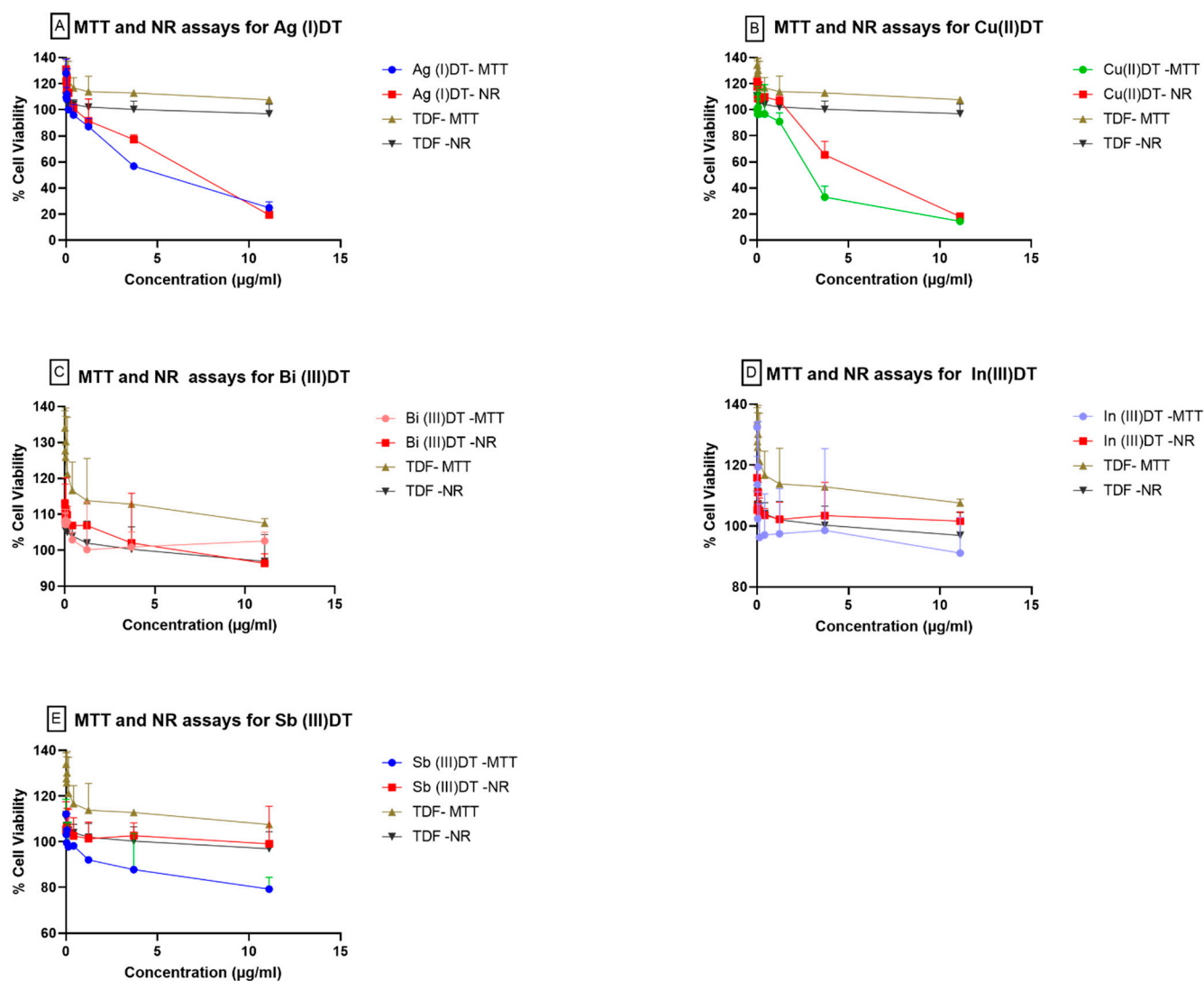

Figure 9. TZM-bl cell viability assessment of *N*-methyl-*N*-phenyl dithiocarbamate complexes of silver(I), bismuth (III), copper (II), indium (III), and antimony (III) using (**A–E**) MTT and neutral red (NR) cytotoxicity assays. The cell viability was determined after 48 h of treatment following a 3-fold serial dilution of the compounds at a starting concentration of 11 µg/mL. TDF was used as a positive control. The assay was performed in triplicate. Error bars indicate the standard deviations.

Furthermore, we evaluated the half-maximal cytotoxic concentration (CC_{50}) of Ag(I)DT and Cu(II)DT (Figure 10) using fit spline/locally weighted scatterplot smoothing (LOWESS) regression [48]. Their CC_{50} was observed to be 3.8 and 3.44 µg/mL, respectively, when tested with the MTT assay and 4.0 and 3.85 µg/mL, respectively, when tested with the neutral red uptake assay, similar to the MTT assay. The other test compounds (Bi(III)DT,

Sb(III)DT, and In(III)DT) did not exhibit any toxicity to the TZM-bl cells, hence the absence of CC_{50} values for these compounds.
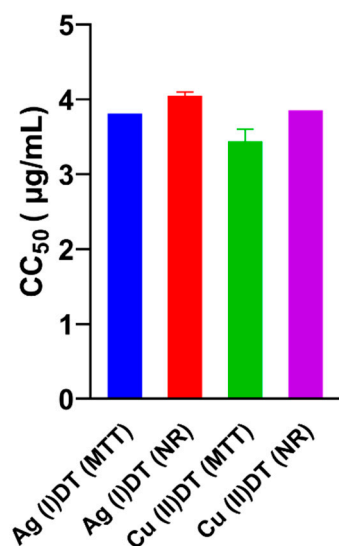

Figure 10. Half-maximal cytotoxic concentration of silver(I) and copper (II) dithiocarbamate complexes in 80% confluent TZM-bl cells. The chemical compounds were used at a starting concentration of 11 µg/mL in both MTT and neutral red (NR) uptake assays.

3.4. Pseudovirus Neutralization Assay

The neutralizing ability of inorganic dithiocarbamate complexes of silver(I), bismuth(III), copper(II), indium(III), and antimony(III) was determined against different subtypes of HIV-1 pseudoviruses (CAP210, ZM53, Q168, and QHO.168) in TZM-bl cells. The gp120 mAb was used as a positive control. A six-point, threefold dilution of the compounds was tested, and the neutralization efficiency of the compounds is shown in Figure 11. Of the five test compounds, two (In(III) and Sb(III)) showed no inhibitory effect against the three different subtypes of HIV-1 that were tested, which suggests that the two complexes have no antiviral effect against HIV-1. Bi(III)DT showed a negligible 15.2% neutralization against the CAP210 HIV-1 subtype C pseudovirus at the highest concentration (11 µg/mL). Of note, Bi(III)DT is a crystalline diamagnetic metal with an established antibacterial effect against a wide range of bacteria [49]. Although the antiviral properties of bismuth and its complexes have not been completely proven, some publications have shown that bismuth complexes can be used as therapeutic agents against SARS-CoV-2 [50,51].

Both Ag(I)DT and Cu(II)DT showed neutralization effects against all the tested HIV-1 subtypes. Their inhibition rates at a concentration of 1.23 µg/mL (the highest concentration where the compounds were non-toxic) were 43% and 94%, respectively, for CAP210; 31% and 54% for ZM53; 13% and 45% for Q168; and 19% and 63% for QHO.168.

The inhibitory effect of gp120 mAb increased with increasing antibody concentration for all the pseudoviruses tested. At the highest concentration of 100 µg/mL, the antibody showed a neutralization effect of 72% for CAP210, 97% for ZM53, 56% for Q168, and 70% for QHO.168, like previous reports [52,53]. The IC_{50} of In(III)DT, Sb(III)DT, and Bi(III)DT could not be reached even at the highest concentration of the complexes. The IC_{50} values of Cu(II)DT against CAP210, ZM53, and QHO.168 were observed as 0.73 µg/mL, 0.93 µg/mL, and 1.06 µg/mL, respectively. The IC_{50} values of HIV-1 gp120 mAb against CAP210, ZM53, Q168, and QHO.168 were 18.7 µg/mL, 25.2 µg/mL, 94.73 µg/mL, and 79.89 µg/mL, respectively (Table 1, Figure 12).

Thus, Cu(II)DT exhibited a strong inhibitory effect against CAP210, followed by ZM53 and QH0.168. This finding further corroborates previous studies reporting that copper (and its alloys) may be used as an antiviral agent [54,55]. Hence, complexes containing this metal might display similar antiviral potential.
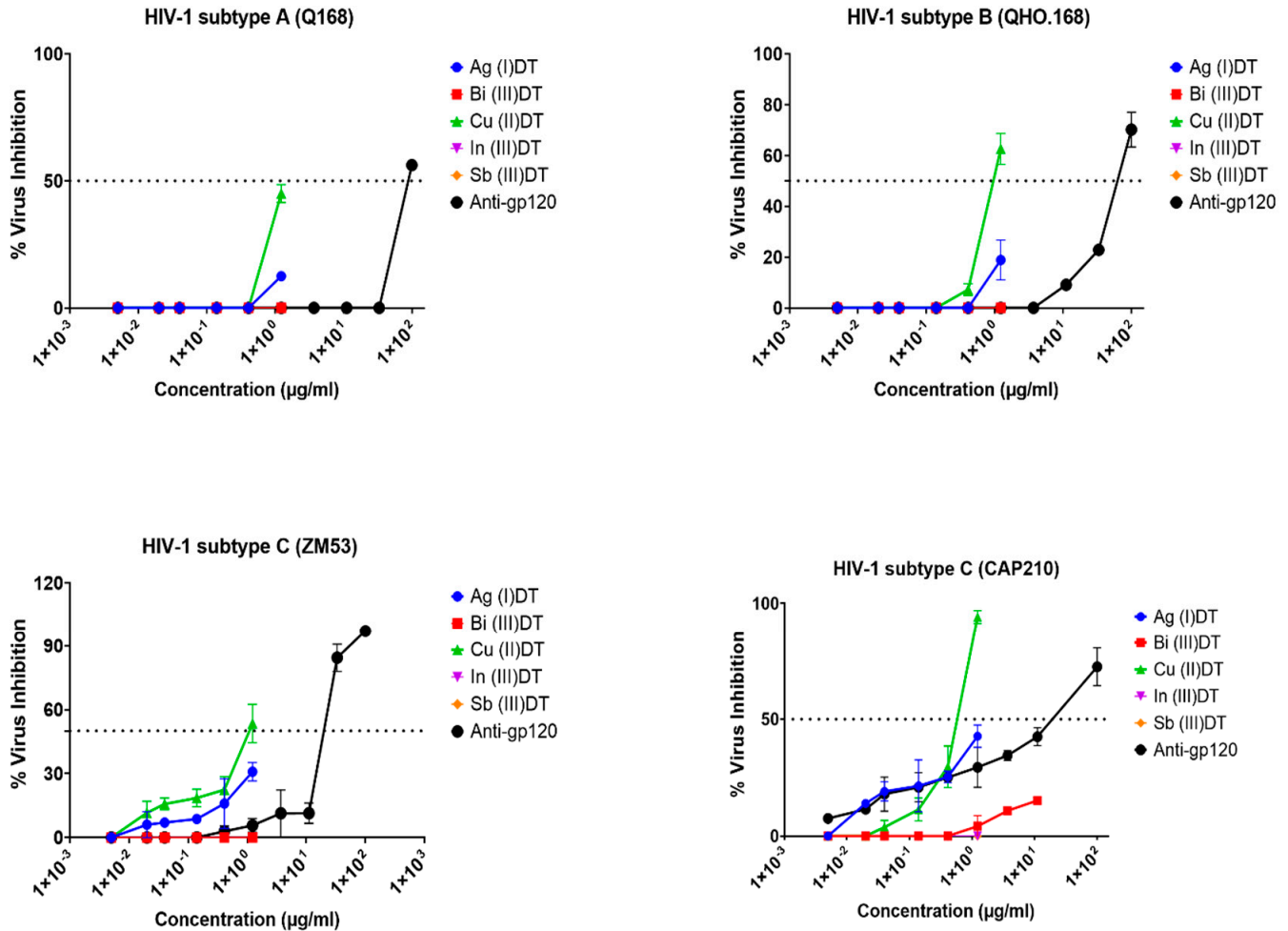

Figure 11. Neutralization assay plot showing the percentage inhibition of different subtypes of HIV-1 Env pseudoviruses with dithiocarbamate complexes of silver(I), bismuth(III), copper(II), indium(III), antimony(III), and gp120 mAb (control) as viral inhibitors. The *x* axis represents inhibitor concentration in μg/mL, and the *y* axis represents percent neutralization. The assay was performed in triplicate. Error bars indicate the mean standard deviations.

Table 1. Neutralization efficiency of Cu(II)DT and gp120 mAb against different subtypes of HIV-1 envelope pseudoviruses.

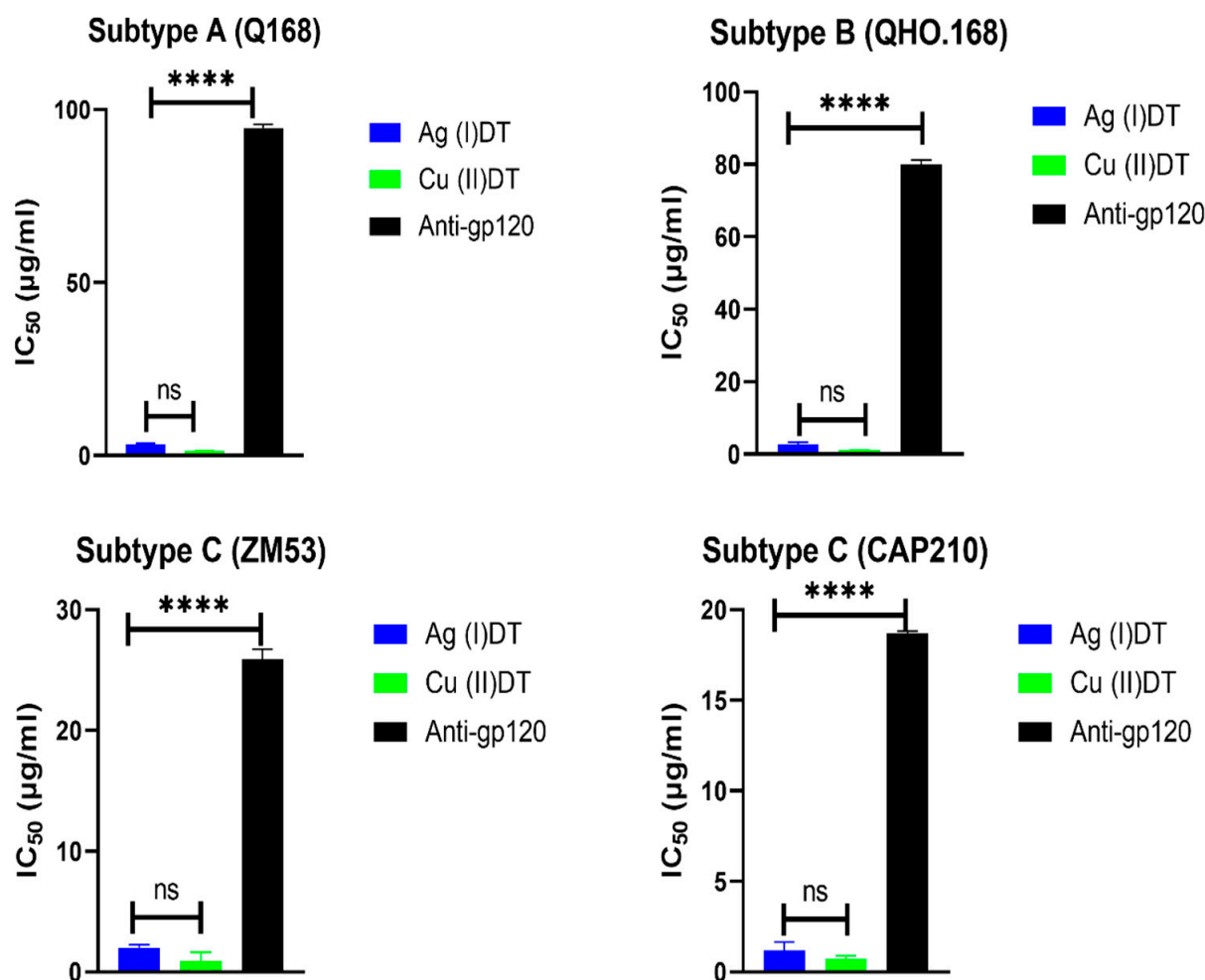| Compound	Pseudovirus	Clade	Accession Number	IC_{50} (μg/mL)	CC_{50} (μg/mL)
Cu (II)DT	ZM53	C	AY423984	0.93	3.44
	CAP210	C	DQ435683	0.73	3.44
	Q168	A	AF407148	1.31	3.44
	QHO.168	B	AY835439	1.06	3.44
Anti-HIV-1 gp120 mAb	ZM53	C	AY423984	25.2	ND
	CAP210	C	DQ435683	18.7	ND
	Q168	A	AF407148	94.73	ND
	QHO.168	B	AY835439	79.89	ND

ND—value not determined.

Figure 12. The half-maximal inhibitory concentration (IC_{50}) of the dithiocarbamate complexes of silver(I) and copper(II) that neutralizes HIV-1 subtypes A, B, and C Env pseudoviruses. A one-way ANOVA test was used to evaluate the statistical differences between the IC_{50} of the compounds. **** $p < 0.0001$; ns means no statistical difference.

4. Conclusions

In this study, *N*-methyl-*N*–phenyl dithiocarbamate complexes of silver(I), bismuth(III), copper(II), indium(III), and antimony(III) were synthesized and characterized, and their antiviral properties were determined against HIV-1 in vitro. The findings revealed that the copper(II)-bis (*N*-methyl-*N*-phenyl dithiocarbamate) complex can be explored for use as a suitable entry inhibitor for HIV. Moreover, the compound could be improved to further enhance its antiviral properties before use as an alternative treatment regimen for HIV. The inhibitory action of the copper dithiocarbamate complex was more pronounced (over 90% inhibition) against HIV-1 subtype C (CAP 210) while it showed less inhibition (>50%) of HIV-1 subtype A (Q168) at a non-toxic concentration of 1.23 µg/mL. Thus, the complex warrants further study on its long-term effects on cells in vitro and in vivo. Moreover, the mechanism of action of these dithiocarbamate complexes against HIV needs to be investigated further.

Author Contributions: H.T.M., O.S.O. and T.O.A. collected data, analyzed the data, and co-authored the draft manuscript. T.O.A. and H.T.M. conceptualized and designed the project. H.T.M., S.D.M. and D.C.O. offered resources and supervision. All authors have read and agreed to the published version of the manuscript.

References

1. Guo, Y.-X.; Liu, M.; Zhou, Y.-Q.; Bi, X.-D.; Gao, F. Terpyridyl ruthenium complexes as visible spectral probe for poly(A) RNA and bifunctional TAR RNA binders and HIV-1 reverse transcriptase inhibitors. *Inorg. Chim. Acta* **2022**, *539*, 121027. [CrossRef]
2. Bahare, S.; Kumar, N.V.A.; Şener, B.; Sharifi-Rad, M.; Kılıç, M.; Mahady, G.B.; Vlaisavljevic, S.; Iriti, M.; Kobarfard, F.; Setzer, W.N.; et al. Medicinal Plants Used in the Treatment of Human Immunodeficiency Virus. *Int. J. Mol. Sci.* **2018**, *19*, 1459.
3. Maina, E.; Adan, A.; Mureithi, H.; Muriuki, J.; Lwembe, R. A review of current strategies towards the elimination of latent HIV-1 and subsequent hiv-1 cure. *Curr. HIV Res.* **2021**, *19*, 14–26. [PubMed]
4. Sun, R.W.-Y.; Ma, D.-L.; Wong, E.L.-M.; Che, C.-M. Some uses of transition metal complexes as anti-cancer and anti-HIV agents. *Dalton Trans.* **2007**, *43*, 4884–4892.
5. de Los Rios, P.; Okoli, C.; Castellanos, E.; Allan, B.; Young, B.; Brough, G.; Muchenje, M.; Eremin, A.; Corbelli, G.M.; McBritton, M. Physical, emotional, and psychosocial challenges associated with daily dosing of HIV medications and their impact on indicators of quality of life: Findings from the positive perspectives study. *AIDS Behav.* **2021**, *25*, 961–972. [CrossRef]
6. Obisesan, O.; Katata-Seru, L.; Mufamadi, S.; Mufhandu, H. Applications of nanoparticles for herpes simplex virus (HSV) and human immunodeficiency virus (HIV) treatment. *J. Biomed. Nanotechnol.* **2021**, *17*, 793–808. [CrossRef]
7. Behzad, F.; Kalyani, F.N.; Samadi, A.; Adabi, M. A promising treatment for HIV-1 using biosynthesis of metal nanoparticles. *J. Ind. Eng. Chem.* **2022**, *115*, 20–25. [CrossRef]
8. Soundararajan, D.; Ramana, L.N.; Shankaran, P.; Krishnan, U.M. Nanoparticle-based strategies to target HIV-infected cells. *Colloids Surf. B Biointerfaces* **2022**, *213*, 112405. [CrossRef]
9. Nakibuuka, M.M.; Mugab, R. Ethnobotanical study of indigenous nutri-medicinal plants used for the management of HIV/AIDS opportunistic ailments among the local communities of central Uganda. *Sci. Afr.* **2022**, *16*, e01245. [CrossRef]
10. Chawuke, P.; van den Berg, N.; Fouche, G.; Maharaj, V.; Shoko, T.; van der Westhuizen, C.J.; Invernizzi, L.; Alexandre, K.B. Lobostemon trigonus (Thunb.) H. Buek, a medicinal plant from South Africa as a potential natural microbicide against HIV-1. *J. Ethnopharmacol.* **2021**, *277*, 114222. [CrossRef]
11. Nyamukuru, A.; Tabuti, J.R.S.; Lamorde, M.; Kato, B.; Sekagya, Y.; Aduma, P.R. Medicinal plants and traditional treatment practices used in the management of HIV/AIDS clients in Mpigi District, Uganda. *J. Herb. Med.* **2017**, *7*, 51–58. [CrossRef]
12. Anywar, G.; Kakudidi, E.; Byamukama, R.; Mukonzo, J.; Schubert, A.; Oryem-Origa, H.; Jassoy, C. A review of the toxicity and phytochemistry of medicinal plant species used by herbalists in treating people living with HIV/AIDS in Uganda. *Front. Pharmacol.* **2021**, *12*, 615147. [CrossRef]
13. Nyakudya, T.T.; Tshabalala, T.; Dangarembizi, R.; Erlwanger, K.H.; Ndhlala, A.R. The Potential Therapeutic Value of Medicinal Plants in the Management of Metabolic Disorders. *Molecules* **2020**, *25*, 2669. [CrossRef] [PubMed]
14. Finamore, A.; Palmery, M.; Bensehaila, S.; Peluso, I. Antioxidant, Immunomodulating, and Microbial-Modulating Activities of the Sustainable and Ecofriendly *Spirulina*. *Oxidative Med. Cell. Longev.* **2017**, *2017*, 3247528. [CrossRef]
15. Mujawdiya, P.K.; Kapur, S. Mangiferin: A potential natural molecule for management of metabolic syndrome. *Int. J. Pharm. Pharm. Sci.* **2015**, *7*, 9–13.
16. Fonteh, P.N.; Keter, F.K.; Meyer, D. New bis(thiosemicarbazonate) gold(III) complexes inhibit HIV replication at cytostatic concentrations: Potential for incorporation into virostatic cocktails. *J. Inorg. Biochem.* **2011**, *105*, 1173–1180. [CrossRef]
17. Duca, M.; Malnuit, V.; Barbault, F.; Benhida, R. Design of novel RNA ligands that bind stem–bulge HIV-1 TAR RNA. *Chem. Commun.* **2010**, *46*, 6162–6164. [CrossRef]
18. Joly, J.-P.; Mata, G.; Eldin, P.; Briant, L.; Fontaine-Vive, F.; Duca, M.; Benhida, R. Artificial Nucleobase–Amino Acid Conjugates: A New Class of TAR RNA Binding Agents. *Chem.—A Eur. J.* **2014**, *20*, 2071–2079. [CrossRef]
19. Wang, M.-F.; Li, Y.; Bi, X.-D.; Guo, Y.-X.; Liu, M.; Zhang, H.; Gao, F. Polypyridyl ruthenium complexes as bifunctional TAR RNA binders and HIV-1 reverse transcriptase inhibitors. *J. Inorg. Biochem.* **2022**, *234*, 111880. [CrossRef]
20. Ajiboye, T.O.; Ajiboye, T.T.; Marzouki, R.; Onwudiwe, D.C. The Versatility in the Applications of Dithiocarbamates. *Int. J. Mol. Sci.* **2022**, *23*, 1317. [CrossRef]
21. Bala, V.; Jangir, S.; Mandalapu, D.; Gupta, S.; Chhonker, Y.S.; Lal, N.; Kushwaha, B.; Chandasana, H.; Krishna, S.; Rawat, K.; et al. Dithiocarbamate–Thiourea Hybrids Useful as Vaginal Microbicides Also Show Reverse Transcriptase Inhibition: Design, Synthesis, Docking and Pharmacokinetic Studies. *Bioorganic Med. Chem. Lett.* **2015**, *25*, 881–886. [CrossRef] [PubMed]
22. Lee, S.A.; Elliott, J.H.; McMahon, J.; Hartogenesis, W.; Bumpus, N.N.; Lifson, J.D.; Savic, R.M. Population Pharmacokinetics and Pharmacodynamics of Disulfiram on Inducing Latent HIV-1 Transcription in a Phase IIb Trial. *Clin. Pharmacol. Ther.* **2019**, *105*, 692–702. [CrossRef] [PubMed]

23. Pang, H.; Chen, D.; Cui, Q.C.; Dou, Q.P. Sodium diethyldithiocarbamate, an AIDS progression inhibitor and a copper-binding compound, has proteasome-inhibitory and apoptosis-inducing activities in cancer cells. *Int. J. Mol. Med.* **2007**, *19*, 809–816. [CrossRef] [PubMed]

24. Takamune, N.; Misumi, S.; Shoji, S. Cyclic Zinc-Dithiocarbamate-S,S'-Dioxide Blocks CXCR4-Mediated HIV-1 Infection1. *Biochem. Biophys. Res. Commun.* **2000**, *272*, 351–356. [CrossRef]

25. Watanabe, K.; Kazakova, I.; Furniss, M.; Miller, S.C. Dual Activity of Pyrrolidine Dithiocarbamate on κB-Dependent Gene Expression in U937 Cells: I. Regulation by the Phorbol Ester TPA. *Cell. Signal.* **1999**, *11*, 479–489. [CrossRef]

26. Schreck, R.; Meier, B.; Männel, D.N.; Dröge, W.; Baeuerle, P.A. Dithiocarbamates as potent inhibitors of nuclear factor kappa B activation in intact cells. *J. Exp. Med.* **1992**, *175*, 1181–1194. [CrossRef] [PubMed]

27. Ajiboye, T.O.; Oluwarinde, B.O.; Montso, P.K.; Ateba, C.N.; Onwudiwe, D.C. Antimicrobial activities of Cu(II), In(III), and Sb(III) complexes of N-methyl-N–phenyl dithiocarbamate complexes. *Results Chem.* **2021**, *3*, 100241. [CrossRef]

28. Ajiboye, T.O.; Oyewo, O.A.; Marzouki, R.; Onwudiwe, D.C. Photocatalytic Reduction of Hexavalent Chromium Using Cu3. 21Bi4. 79S9/g-C3N4 Nanocomposite. *Catalysts* **2022**, *12*, 1075. [CrossRef]

29. Sun, Y.-X.; Song, J.; Kong, L.-J.; Sha, B.-B.; Tian, X.-Y.; Liu, X.-J.; Hu, T.; Chen, P.; Zhang, S.-Y. Design, synthesis and evaluation of novel bis-substituted aromatic amide dithiocarbamate derivatives as colchicine site tubulin polymerization inhibitors with potent anticancer activities. *Eur. J. Med. Chem.* **2022**, *229*, 114069. [CrossRef] [PubMed]

30. Kumar, N.; Venkatesh, R.; Kandasamy, J. Synthesis of functionalized S-benzyl dithiocarbamates from diazo-compounds via multi-component reactions with carbon disulfide and secondary amines. *Org. Biomol. Chem.* **2022**, *20*, 6766–6770. [CrossRef] [PubMed]

31. Li, M.; Gao, F.; Mascola, J.; Stamatatos, L.; Polonis, V.; Koutsoukos, M.; Voss, G.; Goepfert, P.; Gilbert, P.; Greene, K. Human immunodeficiency virus type 1 env clones from acute and early subtype B infections for standardized assessments of vaccine-elicited neutralizing antibodies. *J. Virol.* **2005**, *79*, 10108–10125. [CrossRef] [PubMed]

32. Lei, C.; Yang, J.; Hu, J.; Sun, X. On the calculation of TCID50 for quantitation of virus infectivity. *Virol. Sin.* **2021**, *36*, 141–144. [CrossRef] [PubMed]

33. Vajrabhaya, L.-O.; Korsuwannawong, S. Cytotoxicity evaluation of a Thai herb using tetrazolium (MTT) and sulforhodamine B (SRB) assays. *J. Anal. Sci. Technol.* **2018**, *9*, 1–6. [CrossRef]

34. Ates, G.; Vanhaecke, T.; Rogiers, V.; Rodrigues, R. *Assaying Cellular Viability Using the Neutral Red Uptake Assay, in Cell Viability Assays*; Springer: Berlin/Heidelberg, Germany, 2017; pp. 19–26.

35. Jia, M.; Liberatore, R.; Guo, Y.; Chan, K.-W.; Pan, R.; Lu, H.; Waltari, E.; Mittler, E.; Chandran, K.; Finzi, A. VSV-displayed HIV-1 envelope identifies broadly neutralizing antibodies class-switched to IgG and IgA. *Cell Host Microbe* **2020**, *27*, 963–975.e5. [CrossRef] [PubMed]

36. Li, Y.; Svehla, K.; Louder, M.; Wycuff, D.; Phogat, S.; Tang, M.; Migueles, S.; Wu, X.; Phogat, A.; Shaw, G. Analysis of neutralization specificities in polyclonal sera derived from human immunodeficiency virus type 1-infected individuals. *J. Virol.* **2009**, *83*, 1045–1059. [CrossRef] [PubMed]

37. Onwudiwe, D.C.; Ajibade, P.A. Synthesis, Characterization and Thermal Studies of Zn(II), Cd(II) and Hg(II) Complexes of N-Methyl-N-Phenyldithiocarbamate: The Single Crystal Structure of [(C$_6$H$_5$)(CH$_3$)NCS$_2$]$_4$Hg$_2$. *Int. J. Mol. Sci.* **2011**, *12*, 1964–1978. [CrossRef]

38. Andrew, F.P.; Ajibade, P.A. Synthesis, characterization, and electrochemical studies of Co(II, III) dithiocarbamate complexes. *J. Coord. Chem.* **2019**, *72*, 1171–1186. [CrossRef]

39. Ajiboye, T.O.; Onwudiwe, D.C. Synthesis and Antioxidant Investigation of Ag$_2$S Nanoparticles Obtained from Silver (I) Complex of N-Methyl-N-Phenyl-Dithiocarbamate. *J. Nano Res.* **2022**, *76*, 131–143. [CrossRef]

40. Onwudiwe, D.C.; Nkwe, V.M. Morphological variations in Bi$_2$S$_3$ nanoparticles synthesized by using a single source precursor. *Heliyon* **2020**, *6*, e04505. [CrossRef]

41. Onwudiwe, D.C.; Ajibade, P.A. Synthesis and characterization of metal complexes of N-alkyl-N-phenyl dithiocarbamates. *Polyhedron* **2010**, *29*, 1431–1436. [CrossRef]

42. Singh, R.P.; Maurya, V.K.; Maiti, B.; Siddiqui, K.A.; Prasad, L.B. Synthesis, structure and thermogravimetric analysis of novel dithiocarbamate based Zn(II),Cd(II) and Hg(II) complexes. *J. Mol. Struct.* **2019**, *1198*, 126912. [CrossRef]

43. Chun, U.-K.; Choi, K.; Yang, K.-H.; Park, J.-K.; Song, M.-J. Waste minimization pretreatment via pyrolysis and oxidative pyroylsis of organic ion exchange resin. *Waste Manag.* **1998**, *18*, 183–196. [CrossRef]

44. Onwudiwe, D.C.; Ajibade, P.A. Thermal Studies of Zn(II), Cd(II) and Hg(II) Complexes of Some N-Alkyl-N-Phenyl-Dithiocarbamates. *Int. J. Mol. Sci.* **2012**, *13*, 9502–9513. [CrossRef] [PubMed]

45. Paca, A.M.; Ajibade, P.A. Synthesis and structural studies of iron sulphide nanocomposites prepared from Fe(III) dithiocarbamates single source precursors. *Mater. Chem. Phys.* **2017**, *202*, 143–150. [CrossRef]

46. Nomura, R.; Kanaya, K.; Matsuda, H. Preparation of copper sulfide powders and thin films by thermal decomposition of copper dithiocarbamate complexes. *Ind. Eng. Chem. Res.* **1989**, *28*, 877–880. [CrossRef]

47. Larsson, P.; Engqvist, H.; Biermann, J.; Rönnerman, E.W.; Forssell-Aronsson, E.; Kovács, A.; Karlsson, P.; Helou, K.; Parris, T. Optimization of cell viability assays to improve replicability and reproducibility of cancer drug sensitivity screens. *Sci. Rep.* **2020**, *10*, 1–12. [CrossRef]

48. Kahm, M.; Hasenbrink, G.; Lichtenberg-Fraté, H.; Ludwig, J.; Kschischo, M. Grofit: Fitting biological growth curves. *Nat. Preced.* **2010**, 1. [CrossRef]

49. Alharbi, S.A.; Mashat, B.; Al-Harbi, N.A.; Wainwright, M.; Aloufi, A.; Alnaimat, S. Bismuth-inhibitory effects on bacteria and stimulation of fungal growth in vitro. *Saudi J. Biol. Sci.* **2012**, *19*, 147–150. [CrossRef]

50. Bahrami, A.; Arabestani, M.R.; Taheri, M.; Farmany, A.; Norozzadeh, F.; Hosseini, S.M.; Nouri, F. Exploring the role of heavy metals and their derivatives on the pathophysiology of COVID-19. *Biol. Trace Elem. Res.* **2022**, *200*, 2639–2650. [CrossRef]

51. Yuan, S.; Wang, R.; Chan, J.F.-W.; Zhang, A.J.; Cheng, T.; Chik, K.K.-H.; Ye, Z.-W.; Wang, S.; Lee, A.C.-Y.; Jin, L. Metallodrug ranitidine bismuth citrate suppresses SARS-CoV-2 replication and relieves virus-associated pneumonia in Syrian hamsters. *Nat. Microbiol.* **2020**, *5*, 1439–1448. [CrossRef]

52. Sajadi, M.M.; Dashti, A.; Tehrani, Z.R.; Tolbert, W.; Seaman, M.; Ouyang, X.; Gohain, N.; Pazgier, M.; Kim, D.; Cavet, G. Identification of near-pan-neutralizing antibodies against HIV-1 by deconvolution of plasma humoral responses. *Cell* **2018**, *173*, 1783–1795.e14. [CrossRef] [PubMed]

53. Hioe, C.E.; Wrin, T.; Seaman, M.; Yu, X.; Wood, B.; Self, S.; Williams, C.; Gorny, M.; Zolla-Pazner, S. Anti-V3 monoclonal antibodies display broad neutralizing activities against multiple HIV-1 subtypes. *PLoS ONE* **2010**, *5*, e10254. [CrossRef] [PubMed]

54. Govind, V.; Bharadwaj, S.; Sai Ganesh, M.R.; Vishnu, J.; Shankar, K.V.; Shankar, B.; Rajesh, R. Antiviral properties of copper and its alloys to inactivate COVID-19 virus: A review. *Biometals* **2021**, *34*, 1217–1235. [CrossRef] [PubMed]

55. Jeremiah, S.S.; Miyakawa, K.; Morita, T.; Yamaoka, Y.; Ryo, A. Potent antiviral effect of silver nanoparticles on SARS-CoV-2. *Biochem. Biophys. Res. Commun.* **2020**, *533*, 195–200. [CrossRef] [PubMed]